

SpatialBot: Precise Spatial Understanding with Vision Language Models

Wenxiao Cai^{1,2,3}, Yaroslav Ponomarenko⁴, Jianhao Yuan⁵, Xiaoqi Li⁴,

Wankou Yang⁶, Hao Dong⁴, Bo Zhao^{1,3,*}

¹Shanghai Jiao Tong University ²Stanford University ³BAAI

⁴Peking University ⁵University of Oxford ⁶Southeast University

Abstract—Vision Language Models (VLMs) have achieved impressive performance in 2D image understanding, however they are still struggling with spatial understanding which is the foundation of Embodied AI. In this paper, we propose *SpatialBot* for better spatial understanding by feeding both RGB and depth images. Additionally, we have constructed the *SpatialQA* dataset, which involves multi-level depth-related questions to train VLMs for depth understanding. Finally, we present *SpatialBench* to comprehensively evaluate VLMs’ capabilities in spatial understanding at different levels. Extensive experiments on our spatial-understanding benchmark, general VLM benchmarks and Embodied AI tasks, demonstrate the remarkable improvements of *SpatialBot* trained on *SpatialQA*. The model, code and data are available at <https://github.com/BAAI-DCAI/SpatialBot>.

I. INTRODUCTION

Recently, Vision Language Models (VLMs) [1], [2], [3], [4], [5], [6] have demonstrated notable capabilities in general 2D visual understanding and reasoning, based on the vision-encoder based perception and language-model based reasoning. However, it is still challenging for VLMs to comprehend spatial information from 2D images merely, which plays a significant role in various real-world tasks [7], [8], [9], [10], [11], particularly in the application of embodied AI tasks such as navigation [12], [13], [14], [15] and manipulation [16], [17], [18], [19].

The main challenges for VLMs to have spatial understanding ability are in the following aspects: 1) Current VLMs have limited capacity in understanding depth information as they are only trained on RGB images without depth maps. Consequently, directly inputting depth maps into VLMs results in poor performance. 2) A well-designed dataset for training VLMs to understand depth is absent. The popular VLM tuning datasets do not have corresponding depth maps, meanwhile those depth related tasks do not have question-answering-format data. 3) The inconsistency of the scales between indoor and outdoor numerical depth is also an important problem preventing VLM from uniformly processing depth in various tasks. For example, tasks such as indoor navigation and manipulation require millimeter-level precision, whereas outdoor tasks do not necessitate such high precision but demand a broader depth range.

*Corresponding author: bo.zhao@sjtu.edu.cn.

**This work was done when Wenxiao Cai was a visiting student in SJTU, and when he was an intern in BAAI.

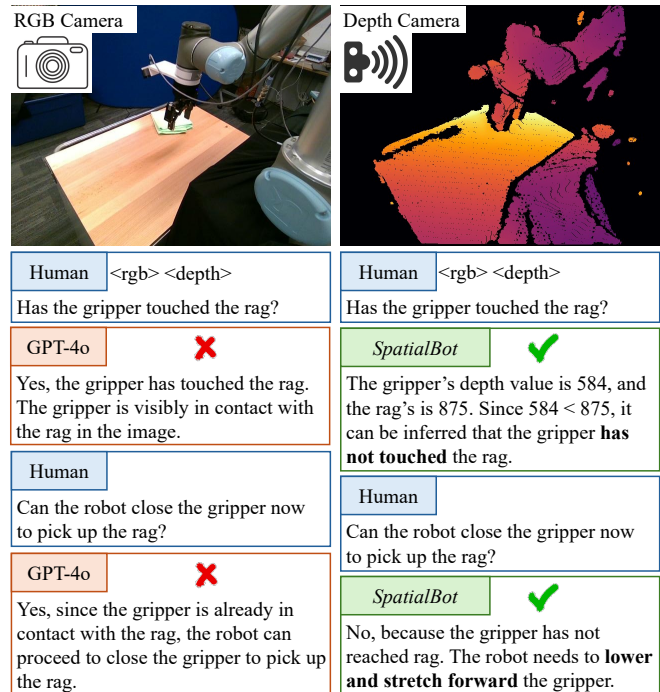


Fig. 1. *SpatialBot* has better spatial understanding ability than GPT-4o. From single RGB image, even human can not judge whether the gripper has touched the rag. GPT-4o fails even if looking at both RGB and depth images. *SpatialBot* first obtains depth information of target objects from the depth map, and then judges that the gripper has not yet touched the rag.

To address these challenges, we propose *SpatialBot* that can precisely comprehend spatial information through depth images, along with the *SpatialQA* dataset for model training. We source from various datasets, including general object recognition (i.e., COCO [20] and Visual Genome [21]) and robot manipulation tasks (i.e., Open X-Embodiment, or RT-X [17]), and introduce a pipeline to extend datasets from RGB to RGB-Depth through a monocular depth estimator. We design various purpose-specific QA tasks that highly rely on spatial understanding from low to high levels. These tasks include the low-level depth estimation, middle-level object detection, referring QA, and depth comparison, and high-level tasks requiring reasoning with depth such as counting, spatial relationship understanding and robot manipulation. To mitigate the problem of indoor-outdoor depth inconsistency, we design an unsigned-integral-24 (uint24) format for nu-

Low-level

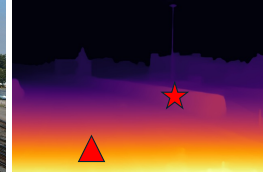
Point Depth: Depth of a single point, directly retrieved from depth map

Q: What is the depth value of point (0.60, 0.58)?

A: point (0.60, 0.58) corresponds to a depth value of ...

Q: What is the depth value of point (0.31, 0.82)?

A: point (0.31, 0.82) corresponds to a depth value of ...



Depth description and analysis

Q: Describe the depth map.

A: The depth map appears to depict an outdoor scene with a ground plane that extends into the distance. There are structures or objects in the middle to upper parts of the image that are further away. A vertical structure, can be seen extending upwards from the middle of the image

Middle-level

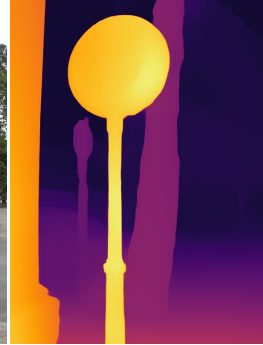
RGB-Depth Alignment: Depth of object, using bounding box or mask

Q: What is the metric depth of object: ROLEX clock?

A: The clock translates to a depth value of 4909, with max depth 5051, min depth 4300, and mean depth 4512.

Q: How far is the pickup truck from the camera?

A: The pickup truck is 17802mm from the camera.



Proximity relationships

Q: Which is closer to the camera, the ROLEX clock, or the pickup truck?

A: The clock has depth value of 4909, while the pickup truck corresponds to a metric depth of 17802, so the ROLEX clock is closer to the camera.

Q: Which appears to be more distant, point (0.62, 0.72) or point (0.39, 0.74)?

A: point (0.62, 0.72) corresponds to a depth of 3312, and point (0.39, 0.74) ...

High-level

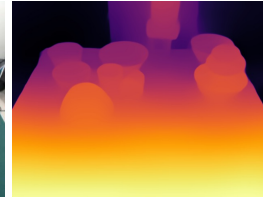
Counting and enumeration

Q: How many orange bowls are there in the image?

A: There are 3 orange bowls.

Q: How many bowls that are upside-down are there in the image?

A: One.



Spatial relationship understanding

Q: Which is closest to the gripper?

A: An orange bowl.

Q: If the red cup is to the right side of the gripper, what is the spatial relationship between the purple cup and gripper?

A: The purple cup is to the left side of gripper, and closer to the camera.

Fig. 2. The proposed *SpatialQA* dataset consists of basic, middle and high level VQAs, aiming to: (a) help VLMs understand depth image, (b) let VLMs learn to align RGB and depth images, (c) enable VLMs to do high-level tasks better by understanding both RGB and depth images, as depth images provide clear boundary information and spatial relationships.

merical depth representation that can preserve the raw depth values and have a broad range of values from 1mm to 131m, in millimeters. To enable the model to accurately obtain depth information, we designed a depth API that allows the model to query the depth values of individual pixels or regions by calling the API.

We validate the capacity of spatial comprehension of VLMs with *SpatialBench* which consists of manually annotated question-answer pairs about spatial understanding and reasoning. The experimental results verify that our *SpatialBot* can better understand the depth in the three levels. Additionally, it is also verified that tuning VLMs on *SpatialQA* can improve their performances on general VLM benchmarks such as MME [22], GQA [23], etc. Finally, we perform robot manipulation tasks in RT-X to demonstrate the promising applications of *SpatialBot*. In summary, the main contributions of our work are as follows:

- We propose *SpatialBot* that shows promising performance in general visual recognition, spatial understanding, and robot manipulation. Especially, *SpatialBot* outperforms GPT-4o [1] in several depth-understanding related tasks.
- We curate a large-scale language-aligned RGB-D question answering dataset, *SpatialQA* for training *SpatialBot* and *SpatialBench* for evaluating VLMs' spatial

understanding performances. Three levels of tasks have been designed for comprehensive analysis.

II. RELATED WORK

A. VLM and RGB datasets

In recent years, VLMs (or Multi-modal Large Language Models, MLLMs) have achieved significant advancements [24]. LLaVA [3] pioneered the visual instruction tuning, which is followed by subsequent works [5], [25], [6], [26], [27] with more extensive datasets [28] and different Large Language Models (LLM) backbones [29], [30], [31], [32]. These VLMs primarily tackle tasks related to perception [22], reasoning [33] and OCR [34], [35]. Additionally, some works have introduced an encoder-decoder structure beyond VLMs to perform pixel-level grounding tasks [36], [37], [38], [39], [40], [41]. However, their performances in counting and enumeration [42], [43] and spatial relationship understanding [44] are mediocre. We posit that comprehending the entire space from a monocular RGB image is overwhelming for VLMs. Integrating depth information could effectively enhance the spatial understanding capabilities of VLMs.

B. Spatial Understanding

Spatial understanding requires VLMs to comprehend scenes beyond 2D RGB images. This is particularly crucial

in precision tasks such as robotic grasping [45]. Spatial understanding can be achieved through point clouds [45], [46] or depth maps [44]. Some studies have attempted to perform depth estimation [47] and 3D detection [48] directly from monocular RGB images, but the accuracy is limited when it comes to metric depth estimation. SpatialVLM [49] infers spatial relationships from 2D images only. However, in robotic tasks (e.g. Fig. 1), depth from sensors is a must in spatial understanding. Recently, Monocular Depth Estimation (MDE) has seen rapid advancements. By utilizing large amounts of unsupervised data [50], [51] and synthetic data [52], MDE can accurately estimate depth in various scenarios [53]. Therefore, we enhance the spatial understanding of VLMs by adding depth information to the RGB images they use, leveraging MDE. Despite the strength of monocular depth estimation models, training large models to estimate depth directly is not always feasible. In embodied AI scenarios, precise depth information is required from hardware devices, which depth estimation models cannot achieve. Additionally, enabling VLMs to precisely understand space from a single RGB image has proven to be exceedingly difficult [48], [47].

III. SPATIALBOT

We use depth information to guide VLMs in understanding space [54], [55], because compared to point clouds, depth information is easier to collect and process. Since the RGB-D cameras are cheap, most of robots carry such cameras to capture RGB and depth images instantly. In addition, due to remarkable capacities of Monocular Depth Estimation (MDE), one can adapt large scale RGB datasets to RGB-D dataset in a fast and affordable way. Thus, we introduce depth images for spatial understanding and construct *SpatialQA* dataset with RGB-D images and depth-related QA pairs. In this section, we elaborate on the pipeline of dataset construction: collecting RGB and depth images, estimating depth images from RGB images using MDE, unifying the format of depth images, generating basic VQAs for VLM training, and generating depth related VQAs. This pipeline can be easily scaled up to construct larger datasets from available RGB datasets.

A. Depth Map Encoding

Our depth encoding aims to preserve all depth information for VLMs to use. A challenge is the indoor and outdoor consistency. Indoor scenes like robot manipulation [17] and indoor navigation [56], [57] may require millimeter-level precision, while outdoor scenes include a large range of depth values. Existing methods often adopt ordinal encoding [58], [50], which, however, cannot be subjected to basic mathematical operations. To address the issue, we use uint24 or three-channel uint8 to store depth values, measured in millimeters from $1mm$ to $131.071m$. We directly save the raw depth values and leave subsequent computations to the powerful fitting capabilities of VLMs. For single-channel uint24, we use millimeter as unit directly. This way, VLMs can directly query the required values from the depth map.

For three-channel uint8 images, we distribute the values across a broader range: the units for the three channels are 2^0 , 2^5 , and 2^{10} millimeters, respectively. Each channel has 2^5 , 2^5 , and 2^7 possible values. For an image of size (H, W) , to store depth value $d_{H,W}$ (in millimeters) in three-channel uint8 image $I_{H,W}^3$, we encode the image I following:

$$I_{h,w}^0 = (d_{h,w} / 2^{10}) * 2^1, \quad (1)$$

$$I_{h,w}^1 = (d_{h,w} / 2^5) * 2^3, \quad (2)$$

$$I_{h,w}^2 = (d_{h,w} \% 2^5) * 2^3. \quad (3)$$

The choice of 2^{10} mm as a unit for the first channel is influenced by the depth range in many desktop grasping tasks in robotics [59], [60], [61], [62], [63], [64], [65], which typically have a maximum depth of around $1m$. A larger unit would result in the first channel being predominantly zero in most scenarios. Similarly, we use multipliers of 2 and 8 to ensure the better distinction between three-channel depth map. We believe VLMs can easily learn the relationship between our encoding method and the actual depth values, and our experiments have validated this.

If the raw data includes depth estimated by sensors, we use the raw depth values. Otherwise, for MDE, we use the ZoeDepth [51] model for estimation, as it considers both indoor and outdoor scenarios and can accurately estimate metric depth in these situations. Note that we do not use the relative depth models, such as MiDaS [53]. It is incorrect to directly take the inverse of the relative depth d_r as the actual depth d . Suppose that the maximum and minimum depth in an image is d_{max} and d_{min} , the conversion should follow:

$$A = \frac{1}{d_{min}} - \frac{1}{d_{max}}, \quad (4)$$

$$B = \frac{1}{d_{max}}, \quad (5)$$

$$d = \frac{1}{(A * d_r + B)}. \quad (6)$$

It is incorrect to ask for the depth value but uses $\frac{1}{d_r}$ as the label in QAs [47]. While $\frac{1}{d_r}$ can reflect the relative size of depth, it does not maintain proportional relationships (e.g. $\frac{1}{d_r} = 0.4$ is not twice the depth of 0.2). Only when the max depth is infinite can $\frac{1}{d_r}$ be considered as true depth multiplies by a scale factor.

B. Depth Description of an Object

SpatialQA is a VQA dataset, and our model is a standard VLM (Fig. 4): it takes images and text as input and outputs text. To maintain generality, we do not use a separate image encoder, so *SpatialBot* cannot output pixel-level information. Intuitively, the center point of objects can simply represent their depth. However, for example, in the case of a cup, there is a significant difference between the depth of the inner and outer surfaces, so a single value cannot accurately represent the depth. Therefore, we use four depth values—max, min, mean, and center—to describe the object’s depth, if its mask is available. Considering that the mask and depth map cannot be perfectly precise, we use the 95th and 5th percentile

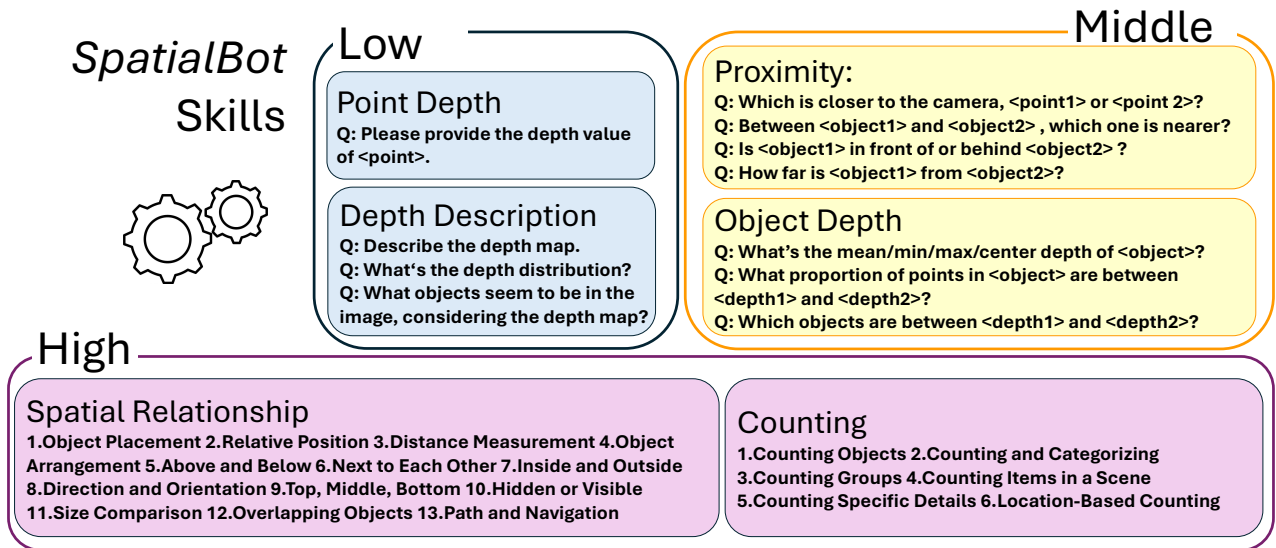


Fig. 3. *SpatialBot* masters three levels of skills: (a) understanding depth images (b) aligning these RGB and depth inputs, and performing proximity comparison, (c) applying RGB-D for spatial relationship understanding and counting.

values as the max and min depth values. If accurate bounding boxes are available, we prompt SAM [66] with the bounding box and its central point to get object masks. If not, we use depth value of the center point of the bounding box.

C. Image Sources

A RGB-D VLM dataset should include detailed QAs that help VLMs to understand the image, which may include reasoning, conversation, description and referring [28]. Specific object descriptions are required, e.g. in Fig. 4, woman is not a good description, but the woman in the middle or the woman standing tallest are good descriptions. Existing captioning, grounding and segmentation models [67], [68], [69], [70] can not generate detailed and specific descriptions. To this end, we base *SpatialQA* mainly on VLM data where detailed QAs are included [6].

In *SpatialQA*, we primarily include three data sources: COCO [20], VG [21], and Open X-Embodiment (RTX) [17]. Therefore, we base our dataset on Bunny_695k [6], which includes COCO and VG. Bunny_695k contains image QA covering reasoning, detailed descriptions, grounding, etc. On this basis, we added depth-related QA pairs. We use bounding boxes in Bunny_695k and prompt SAM [66] with bounding boxes and center points to get masks. We ensure that SAM masks do not exceed the bounding box limits, then select the mask with the highest confidence. RT-X integrates many robotics datasets. For datasets containing sensor depth data, we directly use the raw depth. For other datasets, we use model-estimated metric depth. We select 7.5k of these and manually annotated the bounding boxes, querying the depth information of the objects. For the remaining images, we only ask about the depth of certain pixels in the image. Also, we use GPT-4o to generate conversations based on RTX-7.5k, where we prompt GPT-4o to focus on: what robot are doing, how should the robot finish robot task, object

count, object position, positional relationships and object appearance. In future versions of *SpatialQA*, we will include more images from a vast range of sources.

D. *SpatialQA* Pipeline

To help VLMs understand depth inputs, and use depth information to do high-level tasks like spatial relationship understanding, counting and enumeration, we design a three-step QA pipeline. We aim to make this pipeline effective and easy-to-follow: (a) This pipeline progressively let VLM learn to understand depth, align depth and RGB, and use depth for complex reasoning in high-level tasks. (b) existing RGB datasets can be easily converted to RGB-Depth datasets with our pipeline. *SpatialQA* pipeline is shown in Fig. 5, and the skills to learn are shown in Fig. 3.

Low level. To enable VLMs to understand depth images and learn to query information from them, we ask depth value of points. VLMs should learn to take the depth value directly from depth inputs, and relate point coordinates with pixels in image. In the meanwhile, since the visual encoder does not see depth images in pre-training, we also expect the encoder and projector to learn to encode depth images together with RGB images. We also let *SpatialBot* describe the depth map and infer what may be in the images, giving only a depth map.

Middle level. As VLMs have learnt to encode and query information from depth images, they should now learn to use depth information. Also, since image and depth inputs are given to VLMs, they should also know the relationships between them. First, we ask about proximity relationships, namely which point is closer or further away. Second, we let VLMs learn to describe the depth of objects or regions, by using center point depth, minimum, maximum and mean depth. VLMs should learn to locate an object in the RGB image and then find depth information from depth input.

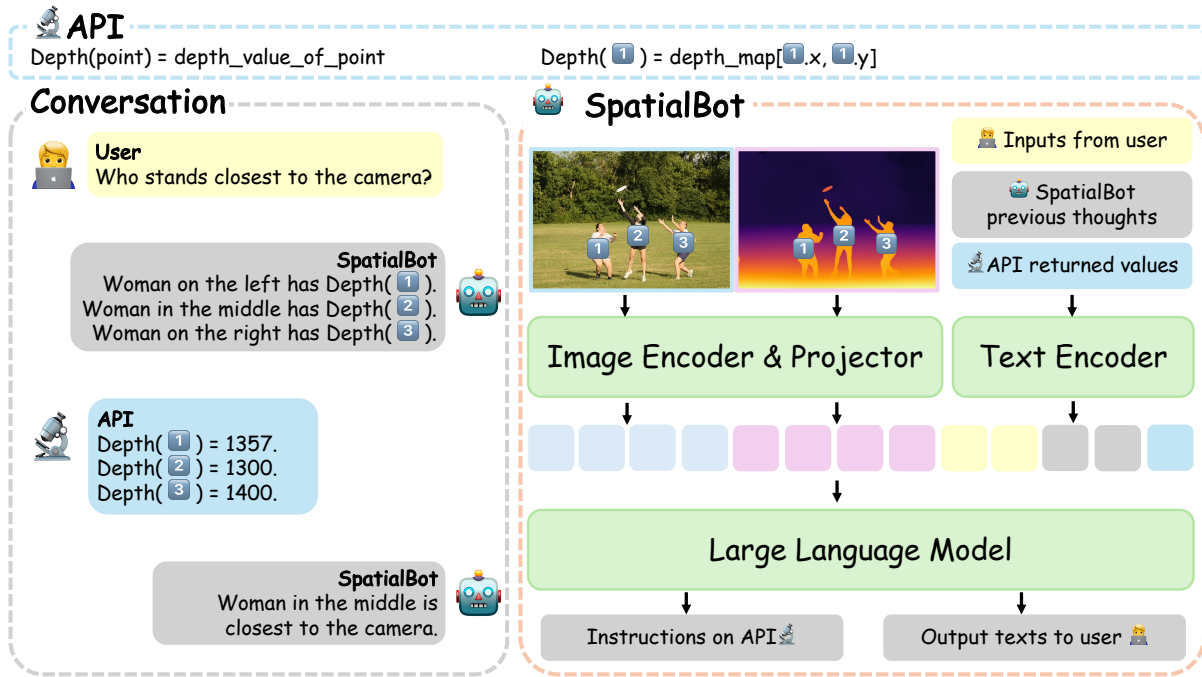


Fig. 4. The architecture of *SpatialBot*. It takes a pair of RGB and depth images as input, where depth images are optional. *SpatialBot* can choose to call Depth API if it need accurate depth information.

Third, we ask about proximity relationships between objects.

High level. Since VLMs can now understand depth input, align depth with RGB and have some knowledge about proximity relationships in the spatial world, we design tasks to help VLMs apply depth at a higher level. When the model sees the depth map, the boundaries of objects and their surroundings become clearer, so we believe that the depth map aids in grounding and counting tasks. Additionally, in *SpatialQA*, the model gains a clear understanding of the space, which helps the model determine spatial and positional relationships.

E. *SpatialBench*

To evaluate VLM’s performance on high-level tasks, we annotate the *SpatialBench*. On 120 images, we ask following questions:

- Has [Object 1] touched/reached [Object 2]?
- What is the spatial relationship between [Object]s?
- Counting and enumeration.
- Size comparison between objects.

All question are in Yes/No or multiple choice formats. Additionally, *SpatialBench* includes depth and proximity questions on images from MME [22] dataset, and our manually annotated 80 images (3 bounding box per image).

F. *SpatialBot* Architecture

SpatialBot uses a VLM structure: Images are processed through an image encoder and a multi-modal projector, converted into tokens, and then sent along with text tokens into an LLM, which ultimately outputs responses. To enable the model to accurately obtain depth information, we designed

Depth API. When the *SpatialBot*’s output contains text with a format of $\text{Depth}(\text{point})$, the API will query the depth value of that point in the corresponding depth map and then input this depth value back into *SpatialBot*. Combining the user’s question with the API’s return value, *SpatialBot* will provide the final answer. The model can call the API to get the precise depth value of a specific point. For example, when *SpatialBot* wants to know the depth information of an object, it first determines the bounding box of the object and then calls the Depth API using the center point of the bounding box. If the model wants to obtain the depth range of this object, it first observes which points in the image correspond to the maximum and minimum depth values and calls the Depth API using the coordinates of these points. However, to enhance the model’s understanding of the depth map itself, during training, we only allow *SpatialBot* to call the API on a subset of the data. For the remaining data, the model must directly use the depth map to answer the depth of the object.

IV. EXPERIMENTS

We start with validating *SpatialBot* has the ability to understand depth, extract information from depth maps, and perform high-level tasks. Then, we observe performance improvements in general VQA tasks, such as MME [22] and GQA [23], by introducing depth maps. This indicates that training on *SpatialQA* can help VLMs perform better on general tasks. Finally, experiments on RT-X [17] show that *SpatialBot* benefits from understanding depth in robot manipulation tasks.

Implementation. We design *SpatialBot* based on Bunny [6], a family of VLMs. Phi-2-3B, Phi-3-4B [30],

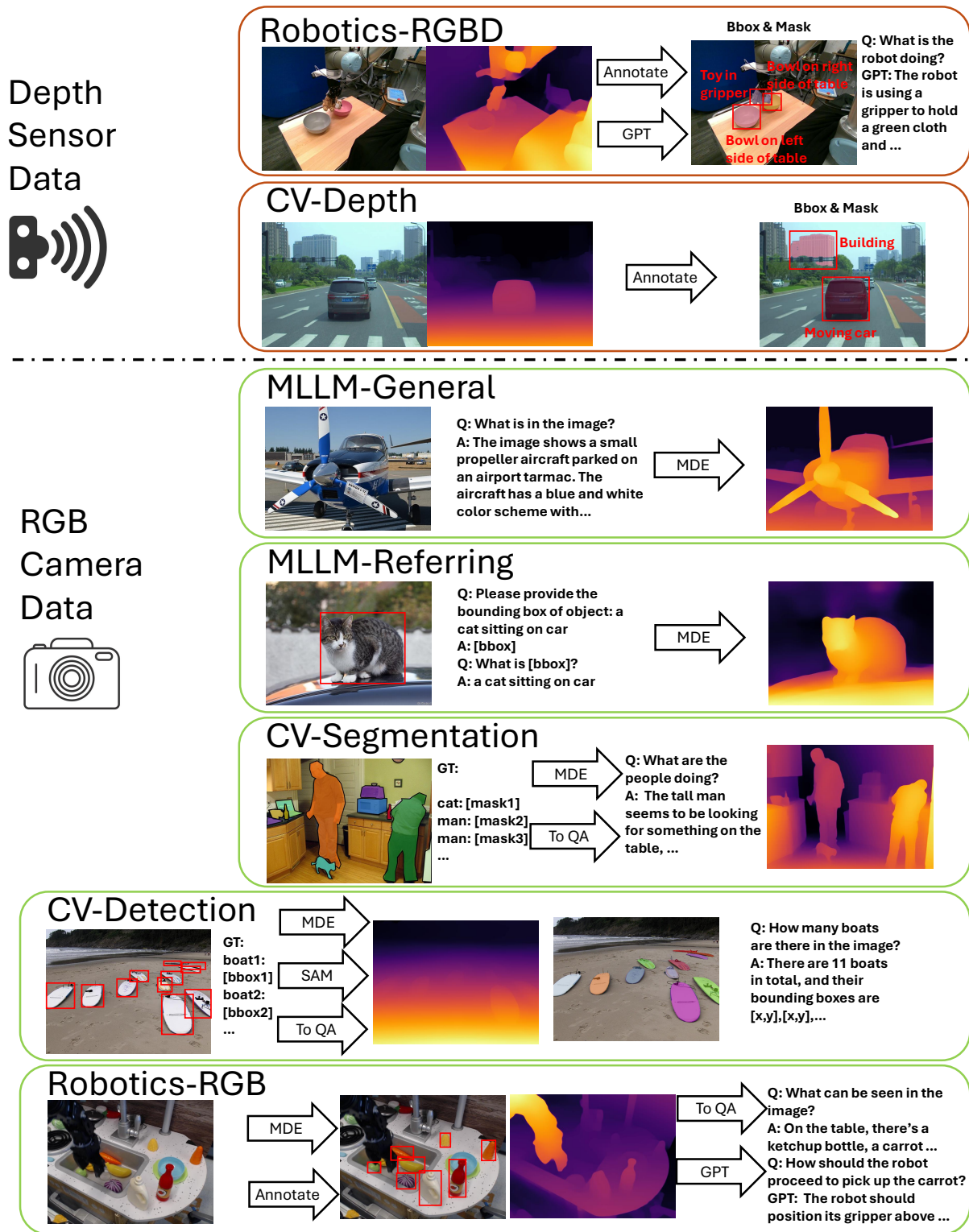


Fig. 5. Image sources and RGB to RGB-Depth dataset conversion pipeline. RGB and depth information, captions or conversations about the images, bounding boxes or masks, and corresponding detailed descriptions of objects are required to make *SpatialQA* dataset.

QWen-1.5-4B [32] and Llama-3-8B [29] are used as the base LLM. *SpatialBot* model architecture is shown in Fig. 4. The image encoder is SigLIP [71] with 384x384 image resolution. QWen-1.5-0.5B and CLIP [72] with 336x336

image resolution are adopted in robot manipulation tasks. We pretrain models on two million image-text pairs from LAION-2B [73] (Bunny-pretrain-LAIION-2M [6]) and finetune them on Bunny_695k [6]. The learning rate is kept

TABLE I

RESULTS ON *SpatialBench*. BEST RESULTS OF MODELS WITH THE SAME BASE LLMs ARE MARKED WITH **BOLD** TEXT. LLM-RGB AND LLM-RGBD ARE TRAINED ON RGB IMAGES ONLY AND TESTED WITH RGB AND RGBD INPUTS, RESPECTIVELY. *SpatialBot* WITH RGB INPUT IN DEPTH ESTIMATION IS THE SAME AS MDE TASK.

Model	Depth \uparrow	Position \uparrow	Existence \uparrow	Counting \uparrow	Reaching \uparrow	Size \uparrow
GPT-4o-RGB	-	70.6	85	84.5	51.7	43.3
GPT-4o-RGBD	-	61.8	90	85.2	51.7	40.0
Bunny-Phi2-3B-RGB	70.6	50.0	75	89.4	51.7	26.7
Bunny-Phi2-3B-RGBD	85.8	50.0	75	90.4	43.3	28.3
<i>SpatialBot</i> -Phi2-3B-RGB	84.1	64.7	80	88.0	61.7	28.3
<i>SpatialBot</i> -Phi2-3B-RGBD	>99	61.8	80	91.7	55	26.7
Bunny-Phi3-4B-RGB	32.3	58.8	75	91.0	31.7	16.7
Bunny-Phi3-4B-RGBD	63.3	52.9	60	85.4	31.7	18.3
<i>SpatialBot</i> -Phi3-4B-RGB	83.2	64.7	75	91.0	40	23.3
<i>SpatialBot</i> -Phi3-4B-RGBD	>99	67.7	70	91.7	35	21.7
QWen-1.5-4B-RGB	42.2	50.0	75	91.6	26.7	15.0
QWen-1.5-4B-RGBD	74.6	44.1	70	90.7	25.0	15.0
<i>SpatialBot</i> -QWen1.5-4B-RGB	89.9	52.9	75	88.6	46.8	18.3
<i>SpatialBot</i> -QWen1.5-4B-RGBD	>99	52.9	60	90.5	41.7	26.7
Llama3-8B-RGB	58.1	50.0	75	91.7	38.3	23.3
Llama3-8B-RGBD	64.0	50.0	75	90.4	38.3	25.0
<i>SpatialBot</i> -Llama3-8B-RGB	85.6	55.9	80	91.2	40.0	20.0
<i>SpatialBot</i> -Llama3-8B-RGBD	>99	53.0	75	90.4	45.0	20.0

TABLE II

RESULTS ON GENERAL VLM BENCHMARKS. FOR SAME BASE LLM MODELS, BETTER RESULTS ARE MARKED WITH **BOLD** TEXT. RGB-D INPUTS ARE ONLY USED IN MME. WE REPORT RESULTS OF MODEL TRAINED WITH RGB AND TESTED WITH RGB OR RGB-D IN IT, SPLIT WITH SLASH.

Model	MME ^P \uparrow	MME ^C \uparrow	MMB ^T \uparrow	MMB ^D \uparrow	SEED-I \uparrow	VQA ^{v2} \uparrow	GQA \uparrow	POPE \uparrow
Bunny-Phi2-3B	1472/1474	286/285	67.90	68.90	69.91	78.98	61.52	86.21
<i>SpatialBot</i> -Phi2-3B	1483/ 1487	310/ 312	70.12	68.56	70.85	79.80	62.28	87.04
Bunny-Phi3-4B	1417/1364	308/319	70.15	70.74	71.04	80.57	61.18	84.60
<i>SpatialBot</i> -Phi3-4B	1431 /1433	337 /329	73.49	73.11	71.64	80.01	62.16	85.47
Bunny-QWen1.5-4B	1340/1364	251/254	69.56	68.56	70.05	80.63	61.55	85.10
<i>SpatialBot</i> -QWen1.5-4B	1378/ 1406	266/ 285	70.91	69.67	70.36	79.69	62.77	86.09
Bunny-Llama3-8B	1574/1542	342/318	73.67	74.15	72.32	80.50	62.18	85.22
<i>SpatialBot</i> -LLama3-8B	1577 /1576	352 /333	75.78	74.83	72.40	80.94	62.90	85.33

$2e-4$, and learning rate for multi-modal projector is $2e-5$, except for Llama-3-8B, where we halve both learning rates. For manipulation tasks, we also halve the learning rate. The multi-modal projector is trainable in both pretrain and finetune stage, and we add a LoRA [74] module in finetuning. We use 8 A100 for training. On *SpatialQA*, it takes about 15 hours for Phi-2 [30].

A. Spatial Understanding

We first validate that *SpatialBot* can get accurate metric depth value from depth images or Depth API, and decide proximity relationships, which are low-level and middle level tasks in *SpatialQA*. We use bounding box and metric depth from *SpatialBench*. We then ask about depth of random points and objects in them. We tell VLMs the names w/ and w/o bounding boxes of target object. For ground truth depth value d_{gt} , estimated depth value d_{est} from VLMs, we estimate depth accuracy by $\frac{d_{gt}-d_{est}}{d_{gt}} * 100\%$. Results by answering with Depth API are shown in Depth and Proximity column in Table. I. Also, we ask the proximity relationships.

B. SpatialBench

We compare model performance on our *SpatialBench*, which composes on positional relationship, object existence, reaching and size comparison tasks. GPT-4o and LLaVA-v1.6-34B [3] without training on *SpatialQA* are compared with models trained on *SpatialQA*. 3B, 4B and 8B models trained on *SpatialQA* reaches comparable results with GPT-4o. Results are reported in Table I.

C. General VLM Benchmarks

We report results on general benchmarks: MME perception [22] (MME^P), MME cognition (MME^C), MM-Bench [33] test and dev set (MMB^T and MMB^D), SEED Bench Image [34] (SEED(-I)), VQA [75] test-dev split (VQA^{v2}), GQA [23], and POPE [76] (the averaged F1-score of three categories on the validation set of COCO). In most of these benchmarks, RGB information along is enough. We only use RGB-Depth input on MME^P and GQA since they contain counting, existence and position questions, where we expect depth information can benefit such cases.

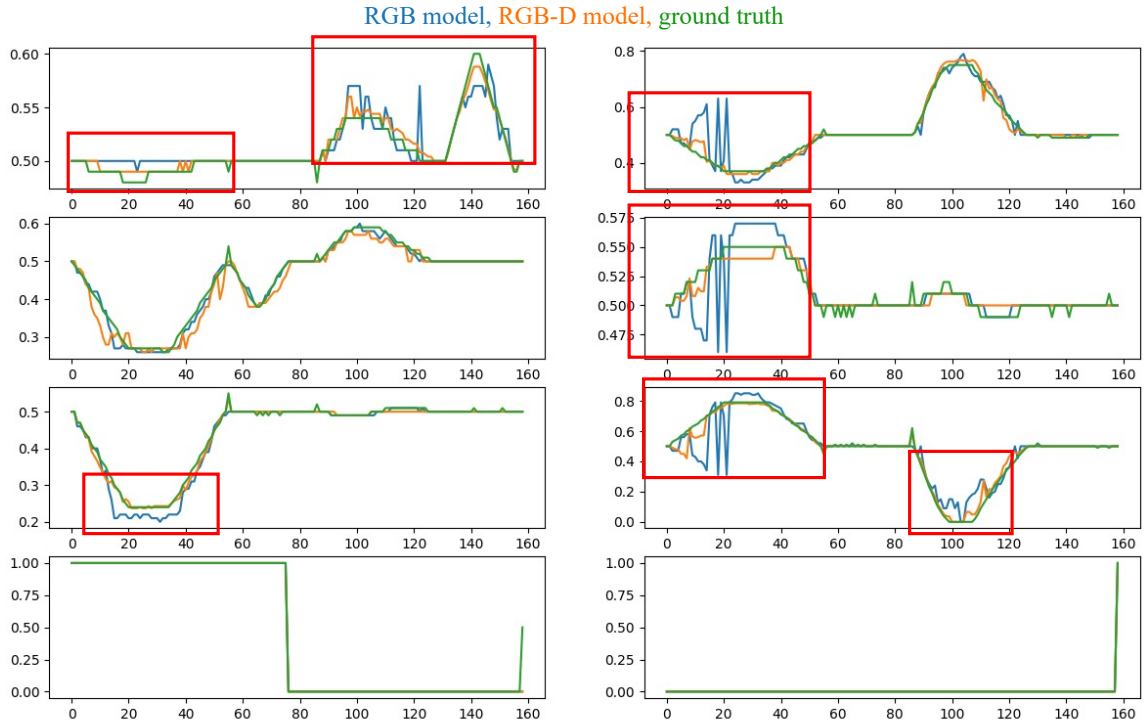


Fig. 6. Results on Maniskill episode 28000. By understanding depth, models can predict robot action better. From left to right, top to down: $(\Delta X, \Delta Y, \Delta Z, \Delta R, \Delta P, \Delta Y_a, C, T)$. x-axis: t , y-axis: encoded control signal.

D. RT-X Robot Manipulation

We test performance of VLMs with and without depth input. Robot manipulations tasks are specified as: in current time stamp t , given history and current image observations $x_{j=0}^t$ (with optional depth maps), models should learn policy $\pi(i, x_{j=0}^t)$. Action a_t is sampled from π and applied to robots. For a robot of two-finger end effector, action space can be $(\Delta X, \Delta Y, \Delta Z, \Delta R, \Delta P, \Delta Y_a, C, T)$, indicating delta change in poses XYZ and rotation RPY_a (roll, pitch, yaw), gripper closure C and whether to terminate action T . The delta change in position and rotation of action space is encoded into 101 possible values, from 0, 0.01 to 1. We use QWen-1.5-0.5B [32] as the base LLM, and CLIP [72] are vision encoder. The pretrain dataset is Bunny-pretrain-LAION-2M, and Maniskill data are used in finetuning. A history of 4 frames are used to predict end-effector delta pose of the current frame. We use Maniskill [77] to evaluate model performance. 7000 episodes are used in training. A sample open-loop control comparison is shown in Fig.6. By understanding depth images, *SpatialBot* can predict robot actions better.

V. CONCLUSION

We propose *SpatialQA* dataset and *SpatialBench* benchmark to train and evaluate *SpatialBot*, a family of state-of-the-art VLMs with real world space knowledge and accurate understanding of depth images. We design QAs to let VLM first query depth information from depth maps, and then use it to compare proximity relationships of points or objects.

We then design high level tasks where depth information may help. Experimental results on our benchmark, general VLM benchmarks, and robot manipulation tasks show that *SpatialBot* can effectively understand and utilize depth information.

SUPPLEMENTARY MATERIAL

I. MONOCULAR DEPTH ESTIMATION BY VLM

We let VLMs to understand depth input so as to get accurate depth information. Readers may wonder that, is MDE for a single point or object difficult? To verify this, we ask *SpatialBot* to predict the depth of points or objects. The results are reported in Table. 1 of main paper (Depth scores of *SpatialBot*-RGB). It seems that VLMs has not been fully prepared for MDE in a text-only output fashion. As reported in [78], [79], [80], [81], an extra decoder may be needed to generate accurate and pixel-level depth. We are not doing so since this new structure limits the generality of SpatialQA.

II. SPATIALBENCH METADATA

In SpatialBench, GPT-4o generate 34 multiple choice questions regarding positional relationships, and we use the correct selection ratio as accuracy. GPT-4o generated 20 positive and negative question pairs on another 20 image. Only when the model answers both the positive and negative questions of a problem correctly is it considered correct. On 20 image, human experts choose a category of object and annotate its quantity. We ask the model to count the objects. Human experts think of positive and negative multiple choice questions regarding whether object A has reached or touched object B, and size comparisons on 20 images respectively. We first calculate the rate of correct choices from models. When it answers a pair of positive and negative questions correctly, we give it a bonus score.

III. DATA GENERATION IN SPATIALQA

We prompt GPT on about 50k images for depthmap understanding, spatial understanding and robot scene understanding in SpatialQA. The data source and data selection protocol are shown in Table. III. GPT prompts we use for three separate tasks are shown in Table. IV. Sample images and generated QAs are shown in Fig. 8, 9, 10, 7. Additionally, human experts annotated 3 bounding boxes per image in RTX, and are asked to annotate gripper if it is clearly visible in the image.

IV. DATASET, MODEL AND BENCHMARK USAGE

The official repository of SpatialBot is <https://github.com/BAAI-DCAI/SpatialBot?tab=readme-ov-file>, where we provide metadata, codes, scripts, checkpoints, licenses and links to resources.

SpatialQA can be downloaded on Hugging Face: <https://huggingface.co/datasets/RussRobin/SpatialQA>.

SpatialBench can be accessed through <https://huggingface.co/datasets/RussRobin/SpatialBench>.

Checkpoint for SpatialBot-3B, which is based on Phi-2 [30] and SigLip [71], can be downloaded at <https://huggingface.co/RussRobin/SpatialBot-3B>.

The pretrained checkpoints of SpatialBot can be accessed through Bunny [6] model zoo: <https://github.com/BAAI-DCAI/Bunny>.

TABLE III

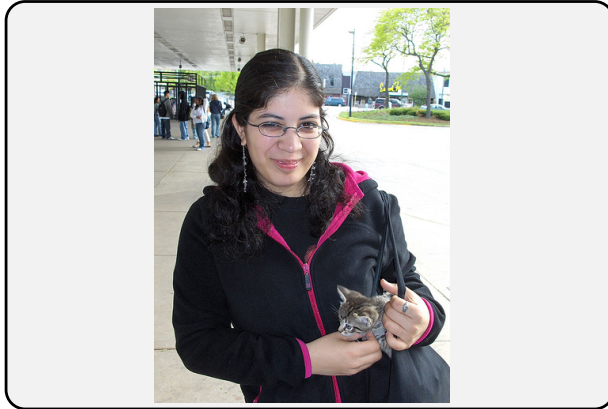
RGB IMAGE AND DEPTH SOURCES IN SPATIALQA. DEPTHMAP IS EITHER FROM SENSORS, AS INCLUDED IN THE ORIGINAL DATASETS, OR MDE DEPTH BY ZOEDEPTH [51].

Data	Aim	Img. Num.	Image Selection Protocol and Depthmap Source
Bunny695k [6]	General MLLM abilities	695k	-
VG, COCO	depthmap understanding	20k	Random selection. GPT is prompted to first infer from the depth color map and then verify its inference against the RGB data to ensure its correctness. The inference of GPT is stored in QA format. MDE.
KITTI [82]	spatial understanding	1.75k	Randomly select images from each sequence of the KITTI dataset. Since some scenes are captured when the car is stationary or temporarily stopped (e.g., at a traffic light or due to a stopped vehicle ahead), there are many repetitive images. We then Manually filter out those with a particularly high repetition rate. Since depth information in KITTI only include sparse points, and ZoeDepth has been finetuned on KITTI, we use MDE.
NYU Depth v2 [83]	spatial understanding	1.5k	All images and sensor depth images are adopted.
RT-X [17]	robot scene understanding	7.5k	We annotate 3 bounding boxes per image, and annotate the gripper if it is visible. We also prompt GPT to generate general QAs. We use depthmap from subsets if available. Otherwise, we use MDE to estimate depth.
SA-1B [66]	spatial understanding	15k	We randomly select real-world images from SA-1B and prompt GPT-4o to generate conversations regarding spatial relationships. MDE.
2D-3D-S [84]	spatial understanding	2.9k	We randomly select images from 2d3ds and manually exclude images with no more than 3 objects in them. Sensor depth.

TABLE IV

GPT PROMPTS USED IN SPATIALQA.

Aim	Prompts for GPT
depthmap understanding	Design a conversation between you and a human talking about the depth map. The human asks you to describe the depth map. You should focus on depth value predictions. The colors just represent depth values. Do not directly mention colors on the image in your response, instead, mention the depth distribution they stand for. Looking at the depth map, you should also infer what may be in the image. If something really exists in the rgb image, and can be inferred from the depth map, you can mention they in your response. If possible, pay attention to spatial relationships. When referring to spatial relationships, such as left and right, you should use the real-world left and right, rather than those in the image coordinate system.
spatial understanding	Design a conversation, consisting of no more than 3 Question-Answer pairs, between you and a person asking about this image. The content within the conversation should be logically connected. You should think of what are spatial relationships of objects in the image. Then generate the conversation according regarding the spatial relationships. Spatial relationships can be about, but not limited to these categories: positional (left/right, below/above, behind/front), distance (further/closer to the camera, further/closer to something), size(big/small, tall/short, wide/thin), reach (has A touched/reached B physically). When describing spatial relationships, always use the real-world orientation as if you are standing in the real scene. e.g. when using right side of object, it should talk about what is on the right side of object in the real world, not on the right side of image'. Only describe the things that you are sure about.
robot scene understanding	Design a conversation, consisting of no more than 3 Question-Answer pairs, between you and a person asking about this image. The content within the conversation should be logically connected. You should first think of robot task: what may the robot want to do with the objects. And then generate the conversation according to robot task. The conversations can include what robot are doing, how should the robot finish robot task, object count, object position, positional relationships, object appearance, etc. Only describe the things that you are sure about. Please note that you are talking to a person about the image and robot. You are not the robot, and you are not talking to the robot.



1. What is the depth value of the woman?

SpatialBot-Phi2-3B: 1241 (GT: 1240)

2. What is the depth value of the cat?

SpatialBot-Phi2-3B : 990 (GT: 987)

3. Which is closer to the camera, cat or woman?

SpatialBot-Phi2-3B : cat corresponds to a depth level of 990, and woman corresponds to a depth level of 1241. Since $990 < 1241$, it can be inferred that: cat is closer to the camera, so the answer is: cat. ✓

Bunny-Phi2-3B : The cat. ✓

Bunny-QWen1.5-4B: They are equally close. ✗

LLaVA-34B: The woman. ✗

GPT-4o: The woman. ✗

4. Where is the cat? Answer with the option's letter from the given choices directly.

- (A) The cat is in the woman's bag.
- (B) The cat is in the woman's pocket.
- (C) The cat is out of the woman's bag.
- (D) The cat is not with the woman.

SpatialBot-Phi2-3B: (A) ✓

Bunny-Phi2-3B : (C) ✗

Bunny-QWen1.5-4B : (C) ✗

LLaVA-34B: (C) ✗

GPT-4o: (A) ✓



1. What is the depth value of the sign?

SpatialBot-Phi2-3B: 4137 (GT: 4137)

2. What is the depth value of the white car?

SpatialBot-Phi2-3B : 28482 (GT: 28479)

3. Which is closer to the camera, sign or white car?

SpatialBot-Phi2-3B : The sign corresponds to a depth measurement of 4137, and the white car corresponds to a depth measurement of 28482. Since $4137 < 28482$, it can be inferred that: the sign is closer to the camera. ✓

Bunny-Phi2-3B : The sign. ✓

Bunny-QWen1.5-4B : The sign. ✓

LLaVA-34B: The sign. ✓

GPT-4o: The sign. ✓

4. What is the arrow of sign pointing to? Answer with the option's letter from the given choices directly.

- (A) The car.
- (B) The grass.
- (C) The sky.
- (D) The building.

SpatialBot-Phi2-3B: (B) ✓

Bunny-Phi2-3B : (A) ✗

Bunny-QWen1.5-4B : (D) ✗

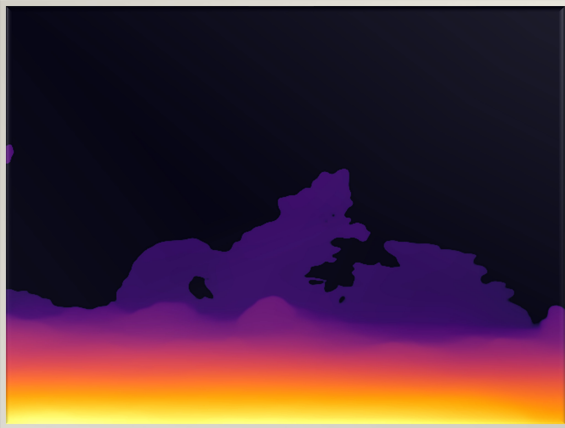
LLaVA-34B: (C) ✗

GPT-4o: (A) ✗

Fig. 7. Sample conversations of *SpatialBot* and baseline models. It first asks about depth value of objects, then lets models compare depth between objects. Finally, spatial relationship questions are asked.

Q: Can you describe the depth map for me?

A: The depth map shows varying depth values across the scene. The bottom portion of the image represents the foreground with the closest depth values, indicating the presence of grass or a field. Towards the middle of the image, there are structures with intermediate depth values suggesting the presence of multiple trees. The upper section depicts the background with the farthest depth values, likely representing the sky. The trees are positioned such that the one to the left is closer than the rightmost one in the scene.



Q: Can you describe the depth map for me?

A: The depth map indicates variations in distance within the scene. The foreground, from the ground plane closest to us, shows the shallowest depth, hinting at the ground level area immediately in front. Further back, shapes that likely represent standing people and possibly objects like posts or bollards can be inferred, with mid-range depth values. Farther back still, we see deeper values, representing a building facade and a vertically elongated structure, probably a lamp post or pole situated in front and towards the middle. It can be inferred that this scene is of a streetscape with people, a sidewalk, and storefronts.

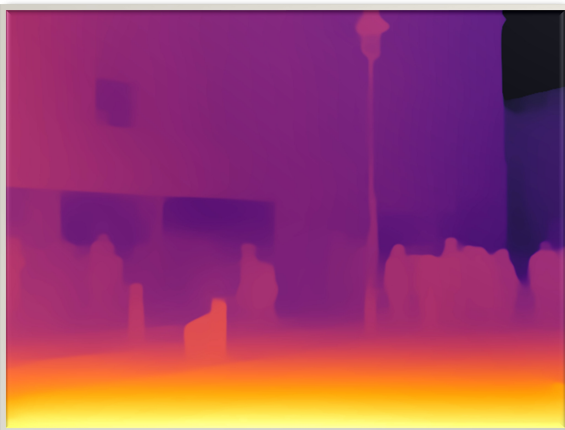


Fig. 8. Sample data of depthmap understanding in *SpatialQA*.

Q1: What can you see on the left side of the canal?

A1: On the left side of the canal, there are several wooden boats docked, a large tree, and some buildings, including garages with closed doors.

Q2: What is the woman in the pink coat walking towards?

A2: The woman in the pink coat is walking along the path that runs parallel to the canal, heading towards the background where more buildings and structures are visible.

Q3: Can you describe the scene on the right side of the canal further up?

A3: Further up on the right side of the canal, there are more boats docked and some trees and buildings in the background. There is also another person walking along the path.



Q1: Which penguin seems to be the tallest?

A1: The penguin sitting on top of the igloo seems to be the tallest.

Q2: Which penguin is the smallest in size?

A2: The penguin on the left, with the red hat, seems to be the smallest in size.

Q3: In the real world, which character is bigger, the igloo or the penguin on top of it?

A3: In the real world, the igloo is bigger than the penguin on top of it.

Q1: Has the yellow car reached the motorcycles?

A1: No, the yellow car has not reached the motorcycles. There is a small gap between them.

Q2: Has anyone reached the area with the red stalls?

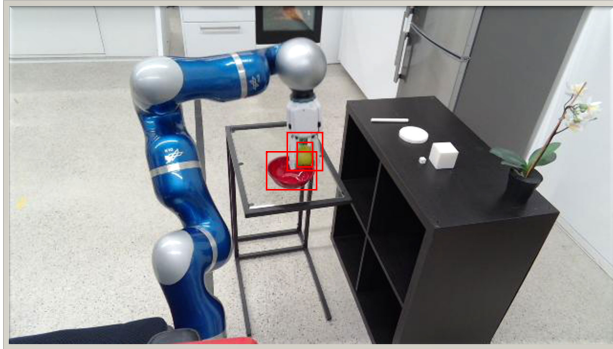
A2: Yes, there are several people around and inside the area with the red stalls.

Q3: Has the white structure near the motorcycles touched any buildings?

A3: No, the white structure near the motorcycles has not touched any buildings. It is standing independently.



Fig. 9. Sample data of spatial understanding in *SpatialQA*.



Q1: What is the robot doing in this image?

A1: The robot appears to be reaching towards two cans placed on a table.

Q2: How many objects are on the table?

A2: There are two cans on the table.

Q3: What is the robot likely trying to do with the cans?

A3: The robot is likely attempting to pick up or move one or both of the cans.

Bounding boxes

Gripper: [0.3,0.117,0.42,0.235],

Can_1: [0.325, 0.147, 0.403, 0.289],

Can_2: [0.232, 0.131, 0.319, 0.3]

Q1: What is the robot doing in this image?

A1: The robot appears to be holding a green object with its gripper arm, placing it on or picking it up from a table.

Q2: What objects are present on the black shelf beside the robot?

A2: There are three objects on the black shelf: a white cylindrical object, a white cube, and a potted plant.

Q3: How should the robot approach picking up the white cube?

A3: The robot should position its gripper arm directly above the white cube, then lower the arm carefully to grip the cube securely before lifting it.

Bounding boxes

Gripper: [0.462, 0.389, 0.514, 0.487],

Bowl: [0.425, 0.443, 0.505, 0.54],

Apple: [0.471, 0.412, 0.499, 0.475]

Fig. 10. Sample data of robot scenes in *SpatialQA*.

REFERENCES

- [1] Z. Yang, L. Li, K. Lin, J. Wang, C.-C. Lin, Z. Liu, and L. Wang, “The dawn of llms: Preliminary explorations with gpt-4v(ision),” *ArXiv*, vol. abs/2309.17421, 2023. [Online]. Available: <https://api.semanticscholar.org/CorpusID:263310951>
- [2] G. Team, R. Anil, S. Borgeaud, Y. Wu, J.-B. Alayrac, J. Yu, R. Soricut, J. Schalkwyk, A. M. Dai, A. Hauth, *et al.*, “Gemini: a family of highly capable multimodal models,” *arXiv preprint arXiv:2312.11805*, 2023.
- [3] H. Liu, C. Li, Q. Wu, and Y. J. Lee, “Visual instruction tuning,” *ArXiv*, vol. abs/2304.08485, 2023. [Online]. Available: <https://api.semanticscholar.org/CorpusID:258179774>
- [4] J. Li, D. Li, S. Savarese, and S. C. H. Hoi, “Blip-2: Bootstrapping language-image pre-training with frozen image encoders and large language models,” in *International Conference on Machine Learning*, 2023. [Online]. Available: <https://api.semanticscholar.org/CorpusID:256390509>
- [5] J. Bai, S. Bai, S. Yang, S. Wang, S. Tan, P. Wang, J. Lin, C. Zhou, and J. Zhou, “Qwen-vl: A versatile vision-language model for understanding, localization, text reading, and beyond,” 2023. [Online]. Available: <https://api.semanticscholar.org/CorpusID:261101015>
- [6] M. He, Y. Liu, B. Wu, J. Yuan, Y. Wang, T. Huang, and B. Zhao, “Efficient multimodal learning from data-centric perspective,” *ArXiv*, vol. abs/2402.11530, 2024. [Online]. Available: <https://api.semanticscholar.org/CorpusID:267751050>
- [7] X. Pan, J. Shi, P. Luo, X. Wang, and X. Tang, “Spatial as deep: Spatial cnn for traffic scene understanding,” in *AAAI Conference on Artificial Intelligence*, 2017. [Online]. Available: <https://api.semanticscholar.org/CorpusID:9164115>
- [8] D. Azuma, T. Miyaniishi, S. Kurita, and M. Kawanabe, “Scanqa: 3d question answering for spatial scene understanding,” *2022 IEEE/CVF Conference on Computer Vision and Pattern Recognition (CVPR)*, pp. 19 107–19 117, 2021. [Online]. Available: <https://api.semanticscholar.org/CorpusID:245334889>
- [9] W. Flores-Fuentes, G. Trujillo-Hernández, I. Y. Alba-Corpus, J. C. Rodríguez-Quiñonez, J. E. Mirada-Vega, D. Hernández-Balbuena, F. N. Murrieta-Rico, and O. Y. Sergiyenko, “3d spatial measurement for model reconstruction: A review,” *Measurement*, 2022. [Online]. Available: <https://api.semanticscholar.org/CorpusID:255331893>
- [10] Z. Kang, J. Yang, Z. Yang, and S. Chong, “A review of techniques for 3d reconstruction of indoor environments,” *ISPRS Int. J. Geo Inf.*, vol. 9, p. 330, 2020. [Online]. Available: <https://api.semanticscholar.org/CorpusID:219492326>
- [11] E. Y. Lam, “Computational photography with plenoptic camera and light field capture: tutorial.” *Journal of the Optical Society of America. A, Optics, image science, and vision*, vol. 32 11, pp. 2021–32, 2015. [Online]. Available: <https://api.semanticscholar.org/CorpusID:28928392>
- [12] S. Levine and D. Shah, “Learning robotic navigation from experience: principles, methods and recent results,” *Philosophical Transactions of the Royal Society B*, vol. 378, 2022. [Online]. Available: <https://api.semanticscholar.org/CorpusID:254564889>
- [13] S. Werner, B. Krieg-Brückner, H. A. Mallot, K. Schweizer, and C. Freksa, “Spatial cognition: The role of landmark, route, and survey knowledge in human and robot navigation,” in *GI Jahrestagung*, 1997. [Online]. Available: <https://api.semanticscholar.org/CorpusID:16607240>
- [14] J. Crespo, J. C. Castillo, Ó. M. Mozos, and R. Barber, “Semantic information for robot navigation: A survey,” *Applied Sciences*, 2020. [Online]. Available: <https://api.semanticscholar.org/CorpusID:214429751>
- [15] J. Yuan, S. Sun, D. Omeiza, B. Zhao, P. Newman, L. Kunze, and M. Gadd, “Rag-driver: Generalisable driving explanations with retrieval-augmented in-context learning in multi-modal large language model,” *arXiv preprint arXiv:2402.10828*, 2024.
- [16] M. Shridhar, L. Manuelli, and D. Fox, “Cliport: What and where pathways for robotic manipulation,” *ArXiv*, vol. abs/2109.12098, 2021. [Online]. Available: <https://api.semanticscholar.org/CorpusID:237396838>
- [17] A. Padalkar, A. Pooley, A. Jain, A. Bewley, A. Herzog, A. Irpan, A. Khazatsky, A. Rai, A. Singh, A. Brohan, *et al.*, “Open x-embodiment: Robotic learning datasets and rt-x models,” *arXiv preprint arXiv:2310.08864*, 2023.
- [18] X. Li, M. Zhang, Y. Geng, H. Geng, Y. Long, Y. Shen, R. Zhang, J. Liu, and H. Dong, “Manipllm: Embodied multimodal large language model for object-centric robotic manipulation,” in *Proceedings of the IEEE/CVF Conference on Computer Vision and Pattern Recognition (CVPR)*, June 2024, pp. 18 061–18 070.
- [19] J. Gao, B. Sarkar, F. Xia, T. Xiao, J. Wu, B. Ichter, A. Majumdar, and D. Sadigh, “Physically grounded vision-language models for robotic manipulation,” *arXiv preprint arXiv:2309.02561*, 2023.
- [20] T.-Y. Lin, M. Maire, S. J. Belongie, J. Hays, P. Perona, D. Ramanan, P. Dollár, and C. L. Zitnick, “Microsoft coco: Common objects in context,” in *European Conference on Computer Vision*, 2014. [Online]. Available: <https://api.semanticscholar.org/CorpusID:14113767>
- [21] R. Krishna, Y. Zhu, O. Groth, J. Johnson, K. Hata, J. Kravitz, S. Chen, Y. Kalantidis, L.-J. Li, D. A. Shamma, M. S. Bernstein, and L. Fei-Fei, “Visual genome: Connecting language and vision using crowdsourced dense image annotations,” *International Journal of Computer Vision*, vol. 123, pp. 32 – 73, 2016. [Online]. Available: <https://api.semanticscholar.org/CorpusID:4492210>
- [22] C. Fu, P. Chen, Y. Shen, Y. Qin, M. Zhang, X. Lin, Z. Qiu, W. Lin, J. Yang, X. Zheng, K. Li, X. Sun, and R. Ji, “Mme: A comprehensive evaluation benchmark for multimodal large language models,” *ArXiv*, vol. abs/2306.13394, 2023. [Online]. Available: <https://api.semanticscholar.org/CorpusID:259243928>
- [23] D. A. Hudson and C. D. Manning, “Gqa: A new dataset for real-world visual reasoning and compositional question answering,” *2019 IEEE/CVF Conference on Computer Vision and Pattern Recognition (CVPR)*, pp. 6693–6702, 2019. [Online]. Available: <https://api.semanticscholar.org/CorpusID:15282269>
- [24] Y. Jin, J. Li, Y. Liu, T. Gu, K. Wu, Z. Jiang, M. He, B. Zhao, X. Tan, Z. Gan, Y. Wang, C. Wang, and L. Ma, “Efficient multimodal large language models: A survey,” *ArXiv*, vol. abs/2405.10739, 2024. [Online]. Available: <https://api.semanticscholar.org/CorpusID:269899856>
- [25] A. Young, B. Chen, C. Li, C. Huang, G. Zhang, G. Zhang, H. Li, J. Zhu, J. Chen, J. Chang, *et al.*, “Yi: Open foundation models by 01. ai,” *arXiv preprint arXiv:2403.04652*, 2024.
- [26] B. McKinzie, Z. Gan, J.-P. Fauconnier, S. Dodge, B. Zhang, P. Duffer, D. Shah, X. Du, F. Peng, F. Weers, *et al.*, “Mml: Methods, analysis & insights from multimodal llm pre-training,” *arXiv preprint arXiv:2403.09611*, 2024.
- [27] Y. Li, Y. Zhang, C. Wang, Z. Zhong, Y. Chen, R. Chu, S. Liu, and J. Jia, “Mini-gemini: Mining the potential of multi-modality vision language models,” *ArXiv*, vol. abs/2403.18814, 2024. [Online]. Available: <https://api.semanticscholar.org/CorpusID:268724012>
- [28] B. Zhao, B. Wu, M. He, and T. Huang, “Svit: Scaling up visual instruction tuning,” *arXiv preprint arXiv:2307.04087*, 2023.
- [29] H. Touvron, T. Lavril, G. Izacard, X. Martinet, M.-A. Lachaux, T. Lacroix, B. Rozière, N. Goyal, E. Hambro, F. Azhar, A. Rodriguez, A. Joulin, E. Grave, and G. Lample, “Llama: Open and efficient foundation language models,” *ArXiv*, vol. abs/2302.13971, 2023. [Online]. Available: <https://api.semanticscholar.org/CorpusID:257219404>
- [30] M. Abidin, S. A. Jacobs, A. A. Awan, J. Aneja, A. Awadallah, H. Awadalla, N. Bach, A. Bahree, A. Bakhtiari, H. Behl, *et al.*, “Phi-3 technical report: A highly capable language model locally on your phone,” *arXiv preprint arXiv:2404.14219*, 2024.
- [31] W.-L. Chiang, Z. Li, Z. Lin, Y. Sheng, Z. Wu, H. Zhang, L. Zheng, S. Zhuang, Y. Zhuang, J. E. Gonzalez, *et al.*, “Vicuna: An open-source chatbot impressing gpt-4 with 90%* chatgpt quality,” *See <https://vicuna.lmsys.org> (accessed 14 April 2023)*, vol. 2, no. 3, p. 6, 2023.
- [32] J. Bai, S. Bai, Y. Chu, Z. Cui, K. Dang, X. Deng, Y. Fan, W. Ge, Y. Han, F. Huang, *et al.*, “Qwen technical report,” *arXiv preprint arXiv:2309.16609*, 2023.
- [33] Y. Liu, H. Duan, Y. Zhang, B. Li, S. Zhang, W. Zhao, Y. Yuan, J. Wang, C. He, Z. Liu, K. Chen, and D. Lin, “Mmbench: Is your multi-modal model an all-around player?” *ArXiv*, vol. abs/2307.06281, 2023. [Online]. Available: <https://api.semanticscholar.org/CorpusID:259837088>
- [34] B. Li, R. Wang, G. Wang, Y. Ge, Y. Ge, and Y. Shan, “Seed-bench: Benchmarking multimodal llms with generative comprehension,” *ArXiv*, vol. abs/2307.16125, 2023. [Online]. Available: <https://api.semanticscholar.org/CorpusID:260334888>

- [35] X. Yue, Y. Ni, K. Zhang, T. Zheng, R. Liu, G. Zhang, S. Stevens, D. Jiang, W. Ren, Y. Sun, C. Wei, B. Yu, R. Yuan, R. Sun, M. Yin, B. Zheng, Z. Yang, Y. Liu, W. Huang, H. Sun, Y. Su, and W. Chen, "Mmmu: A massive multi-discipline multimodal understanding and reasoning benchmark for expert agi," *ArXiv*, vol. abs/2311.16502, 2023. [Online]. Available: <https://api.semanticscholar.org/CorpusID:265466525>
- [36] H. Zhang, H. Li, F. Li, T. Ren, X. Zou, S. Liu, S. Huang, J. Gao, L. Zhang, C. yue Li, and J. Yang, "Llava-grounding: Grounded visual chat with large multimodal models," *ArXiv*, vol. abs/2312.02949, 2023. [Online]. Available: <https://api.semanticscholar.org/CorpusID:265659110>
- [37] H. You, H. Zhang, Z. Gan, X. Du, B. Zhang, Z. Wang, L. Cao, S.-F. Chang, and Y. Yang, "Ferret: Refer and ground anything anywhere at any granularity," *ArXiv*, vol. abs/2310.07704, 2023. [Online]. Available: <https://api.semanticscholar.org/CorpusID:263834718>
- [38] X. Lai, Z. Tian, Y. Chen, Y. Li, Y. Yuan, S. Liu, and J. Jia, "Lisa: Reasoning segmentation via large language model," *ArXiv*, vol. abs/2308.00692, 2023. [Online]. Available: <https://api.semanticscholar.org/CorpusID:260351258>
- [39] Y. Yuan, W. Li, J. Liu, D. Tang, X. Luo, C. Qin, L. Zhang, and J. Zhu, "Osprey: Pixel understanding with visual instruction tuning," *ArXiv*, vol. abs/2312.10032, 2023. [Online]. Available: <https://api.semanticscholar.org/CorpusID:266335219>
- [40] A. Zhang, W. Ji, and T.-S. Chua, "Next-chat: An lmm for chat, detection and segmentation," *ArXiv*, vol. abs/2311.04498, 2023. [Online]. Available: <https://api.semanticscholar.org/CorpusID:265051059>
- [41] J. Yang, R. Ding, E. L. Brown, X. Qi, and S. Xie, "V-irl: Grounding virtual intelligence in real life," *ArXiv*, vol. abs/2402.03310, 2024. [Online]. Available: <https://api.semanticscholar.org/CorpusID:267412337>
- [42] Z. fei Yin, J. Wang, J. Cao, Z. Shi, D. Liu, M. Li, L. Sheng, L. Bai, X. Huang, Z. Wang, W. Ouyang, and J. Shao, "Lamm: Language-assisted multi-modal instruction-tuning dataset, framework, and benchmark," *ArXiv*, vol. abs/2306.06687, 2023. [Online]. Available: <https://api.semanticscholar.org/CorpusID:259138958>
- [43] W. Huang, H. Liu, M. Guo, and N. Z. Gong, "Visual hallucinations of multi-modal large language models," *ArXiv*, vol. abs/2402.14683, 2024. [Online]. Available: <https://api.semanticscholar.org/CorpusID:267782634>
- [44] J. Jain, J. Yang, and H. Shi, "Vcoder: Versatile vision encoders for multimodal large language models," *ArXiv*, vol. abs/2312.14233, 2023. [Online]. Available: <https://api.semanticscholar.org/CorpusID:266521081>
- [45] H. Fang, C. Wang, M. Gou, and C. Lu, "Graspnet-1billion: A large-scale benchmark for general object grasping," *2020 IEEE/CVF Conference on Computer Vision and Pattern Recognition (CVPR)*, pp. 11 441–11 450, 2020. [Online]. Available: <https://api.semanticscholar.org/CorpusID:219964473>
- [46] Z. Xu, C. Gao, Z. Liu, G. Yang, C. Tie, H. Zheng, H. Zhou, W. Peng, D. Wang, T. Chen, Z. Yu, and L. Shao, "Manifoundation model for general-purpose robotic manipulation of contact synthesis with arbitrary objects and robots," 2024. [Online]. Available: <https://api.semanticscholar.org/CorpusID:269757051>
- [47] J. Li, X. Nan, M. Lu, L. Du, and S. Zhang, "Proximity qa: Unleashing the power of multi-modal large language models for spatial proximity analysis," *ArXiv*, vol. abs/2401.17862, 2024. [Online]. Available: <https://api.semanticscholar.org/CorpusID:267334932>
- [48] J. H. Cho, B. Ivanovic, Y. Cao, E. Schmerling, Y. Wang, X. Weng, B. Li, Y. You, P. Krahenbuhl, Y. Wang, and M. Pavone, "Language-image models with 3d understanding," 2024. [Online]. Available: <https://api.semanticscholar.org/CorpusID:269605134>
- [49] B. Chen, Z. Xu, S. Kirmani, B. Ichter, D. Driess, P. Florence, D. Sadigh, L. Guibas, and F. Xia, "Spatialvlm: Endowing vision-language models with spatial reasoning capabilities," *ArXiv*, vol. abs/2401.12168, 2024. [Online]. Available: <https://api.semanticscholar.org/CorpusID:267069344>
- [50] L. Yang, B. Kang, Z. Huang, X. Xu, J. Feng, and H. Zhao, "Depth anything: Unleashing the power of large-scale unlabeled data," *ArXiv*, vol. abs/2401.10891, 2024. [Online]. Available: <https://api.semanticscholar.org/CorpusID:267061016>
- [51] S. Bhat, R. Birkl, D. Wofk, P. Wonka, and M. Muller, "Zoedepth: Zero-shot transfer by combining relative and metric depth," *ArXiv*, vol. abs/2302.12288, 2023. [Online]. Available: <https://api.semanticscholar.org/CorpusID:257205739>
- [52] B. W. Ke, A. Obukhov, S. Huang, N. Metzger, R. C. Daudt, and K. Schindler, "Repurposing diffusion-based image generators for monocular depth estimation," *ArXiv*, vol. abs/2312.02145, 2023. [Online]. Available: <https://api.semanticscholar.org/CorpusID:265609019>
- [53] R. Ranftl, K. Lasinger, D. Hafner, K. Schindler, and V. Koltun, "Towards robust monocular depth estimation: Mixing datasets for zero-shot cross-dataset transfer," *IEEE Transactions on Pattern Analysis and Machine Intelligence*, vol. 44, pp. 1623–1637, 2019. [Online]. Available: <https://api.semanticscholar.org/CorpusID:195776274>
- [54] S. Izadi, D. Kim, O. Hilliges, D. Molyneaux, R. A. Newcombe, P. Kohli, J. Shotton, S. Hodges, D. Freeman, A. J. Davison, and A. W. Fitzgibbon, "Kinectfusion: real-time 3d reconstruction and interaction using a moving depth camera," *Proceedings of the 24th annual ACM symposium on User interface software and technology*, 2011. [Online]. Available: <https://api.semanticscholar.org/CorpusID:3345516>
- [55] H. Pan, T. Guan, Y. Luo, L. Duan, Y. Tian, L. Yi, Y. Zhao, and J. Yu, "Dense 3d reconstruction combining depth and rgb information," *Neurocomputing*, vol. 175, pp. 644–651, 2016. [Online]. Available: <https://api.semanticscholar.org/CorpusID:38137926>
- [56] G. L. Blanc, Y. Mezouar, and P. Martinet, "Indoor navigation of a wheeled mobile robot along visual routes," *Proceedings of the 2005 IEEE International Conference on Robotics and Automation*, pp. 3354–3359, 2005. [Online]. Available: <https://api.semanticscholar.org/CorpusID:17799387>
- [57] F. Gul, W. Rahiman, and S. S. N. Alhady, "A comprehensive study for robot navigation techniques," *Cogent Engineering*, vol. 6, 2019. [Online]. Available: <https://api.semanticscholar.org/CorpusID:198355741>
- [58] H. Fu, M. Gong, C. Wang, K. Batmanghelich, and D. Tao, "Deep ordinal regression network for monocular depth estimation," *2018 IEEE/CVF Conference on Computer Vision and Pattern Recognition*, pp. 2002–2011, 2018. [Online]. Available: <https://api.semanticscholar.org/CorpusID:46968214>
- [59] L. Y. Chen, S. Adebola, and K. Goldberg, "Berkeley UR5 demonstration dataset," <https://sites.google.com/view/berkeley-ur5/home>.
- [60] H. Walke, K. Black, A. Lee, M. J. Kim, M. Du, C. Zheng, T. Zhao, P. Hansen-Estruch, Q. H. Vuong, A. W. He, V. Myers, K. Fang, C. Finn, and S. Levine, "Bridgedata v2: A dataset for robot learning at scale," in *Conference on Robot Learning*, 2023. [Online]. Available: <https://api.semanticscholar.org/CorpusID:261100981>
- [61] Y. Feng, N. Hansen, Z. Xiong, C. Rajagopalan, and X. Wang, "Finetuning offline world models in the real world," *ArXiv*, vol. abs/2310.16029, 2023. [Online]. Available: <https://api.semanticscholar.org/CorpusID:264438898>
- [62] H. Shi, H. Xu, S. Clarke, Y. Li, and J. Wu, "Robocook: Long-horizon elasto-plastic object manipulation with diverse tools," *ArXiv*, vol. abs/2306.14447, 2023. [Online]. Available: <https://api.semanticscholar.org/CorpusID:259251806>
- [63] Y. Wang, Z. Li, M. Zhang, K. Driggs-Campbell, J. Wu, L. Fei-Fei, and Y. Li, "D3fields: Dynamic 3d descriptor fields for zero-shot generalizable robotic manipulation," *ArXiv*, vol. abs/2309.16118, 2023. [Online]. Available: <https://api.semanticscholar.org/CorpusID:263134320>
- [64] A. Khazatsky, K. Pertsch, S. Nair, A. Balakrishna, S. Dasari, S. Karamcheti, S. Nasiriany, M. K. Srirama, L. Y. Chen, K. Ellis, et al., "Droid: A large-scale in-the-wild robot manipulation dataset," *arXiv preprint arXiv:2403.12945*, 2024.
- [65] Y. Jiang, A. Gupta, Z. Zhang, G. Wang, Y. Chen, L. Fei-Fei, A. Anandkumar, Y. Zhu, and L. J. Fan, "Vima: General robot manipulation with multimodal prompts," *ArXiv*, vol. abs/2210.03094, 2022. [Online]. Available: <https://api.semanticscholar.org/CorpusID:252735175>
- [66] A. Kirillov, E. Mintun, N. Ravi, H. Mao, C. Rolland, L. Gustafson, T. Xiao, S. Whitehead, A. C. Berg, W.-Y. Lo, P. Dollár, and R. B. Girshick, "Segment anything," *2023 IEEE/CVF International Conference on Computer Vision (ICCV)*, pp. 3992–4003, 2023. [Online]. Available: <https://api.semanticscholar.org/CorpusID:257952310>
- [67] S. Liu, Z. Zeng, T. Ren, F. Li, H. Zhang, J. Yang, C. yue Li, J. Yang, H. Su, J.-J. Zhu, and L. Zhang, "Grounding dino: Marrying dino with grounded pre-training for open-set object detection," *ArXiv*, vol. abs/2303.05499, 2023. [Online]. Available: <https://api.semanticscholar.org/CorpusID:257427307>
- [68] T. Cheng, L. Song, Y. Ge, W. Liu, X. Wang, and Y. Shan, "Yolo-world: Real-time open-vocabulary object detection," *ArXiv*, vol. abs/2401.17270, 2024. [Online]. Available: <https://api.semanticscholar.org/CorpusID:267320681>

- [69] T. Ren, S. Liu, A. Zeng, J. Lin, K. Li, H. Cao, J. Chen, X. Huang, Y. Chen, F. Yan, Z. Zeng, H. Zhang, F. Li, J. Yang, H. Li, Q. Jiang, and L. Zhang, "Grounded sam: Assembling open-world models for diverse visual tasks," *ArXiv*, vol. abs/2401.14159, 2024. [Online]. Available: <https://api.semanticscholar.org/CorpusID:267212047>
- [70] X. Zou, J. Yang, H. Zhang, F. Li, L. Li, J. Gao, and Y. J. Lee, "Segment everything everywhere all at once," *ArXiv*, vol. abs/2304.06718, 2023. [Online]. Available: <https://api.semanticscholar.org/CorpusID:258108410>
- [71] X. Zhai, B. Mustafa, A. Kolesnikov, and L. Beyer, "Sigmoid loss for language image pre-training," *2023 IEEE/CVF International Conference on Computer Vision (ICCV)*, pp. 11 941–11 952, 2023. [Online]. Available: <https://api.semanticscholar.org/CorpusID:257767223>
- [72] A. Radford, J. W. Kim, C. Hallacy, A. Ramesh, G. Goh, S. Agarwal, G. Sastry, A. Askell, P. Mishkin, J. Clark, G. Krueger, and I. Sutskever, "Learning transferable visual models from natural language supervision," in *International Conference on Machine Learning*, 2021. [Online]. Available: <https://api.semanticscholar.org/CorpusID:231591445>
- [73] C. Schuhmann, R. Beaumont, R. Vencu, C. Gordon, R. Wightman, M. Cherti, T. Coombes, A. Katta, C. Mullis, M. Wortsman, P. Schramowski, S. Kundurthy, K. Crowson, L. Schmidt, R. Kaczmarczyk, and J. Jitsev, "Laion-5b: An open large-scale dataset for training next generation image-text models," *ArXiv*, vol. abs/2210.08402, 2022. [Online]. Available: <https://api.semanticscholar.org/CorpusID:252917726>
- [74] J. E. Hu, Y. Shen, P. Wallis, Z. Allen-Zhu, Y. Li, S. Wang, and W. Chen, "Lora: Low-rank adaptation of large language models," *ArXiv*, vol. abs/2106.09685, 2021. [Online]. Available: <https://api.semanticscholar.org/CorpusID:235458009>
- [75] Y. Goyal, T. Khot, D. Summers-Stay, D. Batra, and D. Parikh, "Making the v in vqa matter: Elevating the role of image understanding in visual question answering," *International Journal of Computer Vision*, vol. 127, pp. 398 – 414, 2016. [Online]. Available: <https://api.semanticscholar.org/CorpusID:8081284>
- [76] Y. Li, Y. Du, K. Zhou, J. Wang, W. X. Zhao, and J. rong Wen, "Evaluating object hallucination in large vision-language models," in *Conference on Empirical Methods in Natural Language Processing*, 2023. [Online]. Available: <https://api.semanticscholar.org/CorpusID:258740697>
- [77] J. Gu, F. Xiang, X. Li, Z. Ling, X. Liu, T. Mu, Y. Tang, S. Tao, X. Wei, Y. Yao, X. Yuan, P. Xie, Z. Huang, R. Chen, and H. Su, "Maniskill2: A unified benchmark for generalizable manipulation skills," *ArXiv*, vol. abs/2302.04659, 2023. [Online]. Available: <https://api.semanticscholar.org/CorpusID:256697500>
- [78] Z. Zeng, D. Wang, F. Yang, H. Park, Y. Wu, S. Soatto, B.-W. Hong, D. Lao, and A. Wong, "Wordepth: Variational language prior for monocular depth estimation," *ArXiv*, vol. abs/2404.03635, 2024. [Online]. Available: <https://api.semanticscholar.org/CorpusID:268889577>
- [79] D. Auty and K. Mikolajczyk, "Language-based depth hints for monocular depth estimation," *ArXiv*, vol. abs/2403.15551, 2024. [Online]. Available: <https://api.semanticscholar.org/CorpusID:268680420>
- [80] R. Zhang, Z. Zeng, and Z. Guo, "Can language understand depth?" *Proceedings of the 30th ACM International Conference on Multimedia*, 2022. [Online]. Available: <https://api.semanticscholar.org/CorpusID:250264495>
- [81] D. Auty and K. Mikolajczyk, "Learning to prompt clip for monocular depth estimation: Exploring the limits of human language," *2023 IEEE/CVF International Conference on Computer Vision Workshops (ICCVW)*, pp. 2031–2049, 2023. [Online]. Available: <https://api.semanticscholar.org/CorpusID:264131865>
- [82] J. Uhrig, N. Schneider, L. Schneider, U. Franke, T. Brox, and A. Geiger, "Sparsity invariant cnns," *2017 International Conference on 3D Vision (3DV)*, pp. 11–20, 2017. [Online]. Available: <https://api.semanticscholar.org/CorpusID:206429195>
- [83] N. Silberman, D. Hoiem, P. Kohli, and R. Fergus, "Indoor segmentation and support inference from rgbd images," in *European Conference on Computer Vision*, 2012. [Online]. Available: <https://api.semanticscholar.org/CorpusID:545361>
- [84] I. Armeni, S. Sax, A. Zamir, and S. Savarese, "Joint 2d-3d-semantic data for indoor scene understanding," *ArXiv*, vol. abs/1702.01105, 2017. [Online]. Available: <https://api.semanticscholar.org/CorpusID:2730848>